ChemBioChem

Research Article
doi.org/10.1002/cbic.202200635

Chemistry Europe
European Chemical Societies Publishing

www.chembiochem.org

VIP *Very Important Paper*

Myxococcus xanthus as Host for the Production of Benzoxazoles

Lea Winand,[a] Lucia Lernoud,[a] Saskia Anna Meyners,[a] Katharina Kuhr,[a] Wolf Hiller,[b] and Markus Nett*[a]

Benzoxazoles are important structural motifs in pharmaceutical drugs. Here, we present the heterologous production of 3-hydroxyanthranilate-derived benzoxazoles in the host bacterium *Myxococcus xanthus* following the expression of two genes from the nataxazole biosynthetic gene cluster of *Streptomyces* sp. Tü 6176. The *M. xanthus* expression strain achieved a benzoxazole titer of 114.6 ± 7.4 mg L^{-1} upon precursor supplementation, which is superior to other bacterial production systems. Crosstalk between the heterologously expressed benzoxazole pathway and the endogenous myxochelin pathway led to the combinatorial biosynthesis of benzoxazoles featuring a 2,3-dihydroxybenzoic acid (2,3-DHBA) building block. Subsequent in vitro studies confirmed that this crosstalk is not only due to the availability of 2,3-DHBA in *M. xanthus*, rather, it is promoted by the adenylating enzyme MxcE from the myxochelin pathway, which contributes to the activation of aryl carboxylic acids and delivers them to benzoxazole biosynthesis.

Introduction

Several pharmaceutical drugs incorporate one or more heterocyclic substructures. These moieties often contribute to the biological activity of the drug as part of the pharmacophore. Furthermore, they influence the physicochemical properties as well as the bioavailability.[1] For that reason, the synthesis of heterocyclic compounds and their functionalization has been addressed in an impressive number of studies.[2]

Nature has developed diverse biosynthetic routes for the synthesis of heterocycles by way of enzymes such as polyketide synthases, nonribosomal peptide synthetases, cyclodipeptide synthases or Pictet-Spenglerases.[3] Recently, some members of the amidohydrolase superfamily were reported to catalyze heterocyclizations. In the biosynthesis of the anti-inflammatory natural product pseudochelin A, the amidohydrolase MxcM condenses a β-aminoethyl amide residue to generate an imidazoline moiety.[4,5] A similar mechanism was described in the biosynthesis of benzoxazoles. Upon enzymatic linkage of 3-hydroxyanthranilic acid (3-HAA) with another aryl carboxylic acid via an ester bond, an amidohydrolase catalyzes the formation of a hemiorthoamide intermediate and a subsequent dehydration to give a benzoxazole (Figure 1A).[6] Natural products such as the antibiotics caboxamycin and A-33853 or the anticancer agent nataxazole are synthesized in this way (Figure 1B).[6,7] A distinct assembly strategy is pursued in the biosynthesis of the closoxazoles, which were recently identified from the anaerobic bacterium *Clostridium cavendishii* DSM21758.[8] The closoxazole pathway represents the first example of a benzoxazole biosynthetic pathway that utilizes a 3,4-disubstituted aryl carboxylic acid as a building block and, hence, generates *meta*-substituted benzoxazoles.

Benzoxazole-containing compounds are used in different therapeutic areas, as exemplified by the approved drugs chlorzoxazone (muscle relaxant), tafamidis (transthyretin stabilizer) or suvorexant (treatment of insomnia).[9] Their potent biological activities combined with the understanding of benzoxazole biosynthesis have stimulated the biotechnological production of benzoxazole analogs.[6–8,10–12] Recently, the genes involved in nataxazole biosynthesis were expressed in the bacterium *Escherichia coli* and, upon feeding of 3-HAA together with other aryl carboxylic acids, various benzoxazoles were generated, albeit in low titers.[12]

In this study, we describe an alternative heterologous production system for benzoxazoles. As production organism, we chose the myxobacterium *Myxococcus xanthus*. Unlike *E. coli*, *M. xanthus* possesses an endogenous pathway to the benzoxazole building block 3-HAA according to an analysis of the KEGG database.[13] This suggested that the heterologous production of benzoxazoles in *M. xanthus* would not depend on precursor feeding. Furthermore, *M. xanthus* is known to be highly amenable to secondary metabolite biosynthesis. By means of metabolic engineering considerable product titers can be achieved with this host,[14] which was also demonstrated to outcompete *E. coli* in the heterologous production of structurally complex secondary metabolites.[15] More recently, a plasmid-based expression system has been developed, which facilitates the expression of foreign genes in *M. xanthus*.[5] This

[a] L. Winand, L. Lernoud, S. A. Meyners, K. Kuhr, Prof. Dr. M. Nett
Department of Biochemical and Chemical Engineering
Laboratory of Technical Biology, TU Dortmund University
Emil-Figge-Str. 66, 44227 Dortmund (Germany)
E-mail: markus.nett@tu-dortmund.de
[b] Prof. Dr. W. Hiller
Department of Chemistry and Chemical Biology
NMR Laboratory, TU Dortmund University
Otto-Hahn-Str. 4a, 44227 Dortmund (Germany)

Supporting information for this article is available on the WWW under https://doi.org/10.1002/cbic.202200635

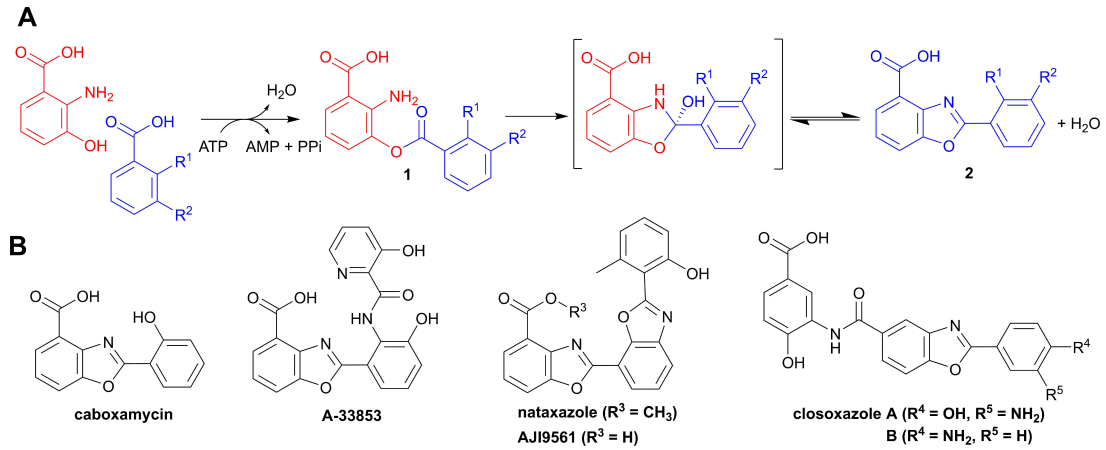

Figure 1. Amidohydrolase-mediated benzoxazole biosynthesis. A) General reaction mechanism. B) Examples of benzoxazole-containing natural products.[6,7]

system was already successfully used not only for the expression of the imidazoline-forming amidohydrolase MxcM, but also for the recombinant production of alkaloids in *M. xanthus*.[16,17] In sum, it was expected that the advantages of *M. xanthus* would outweigh its slower growth in comparison to *E. coli*.

Results and Discussion

Previous studies indicated that only two enzymes are required for benzoxazole biosynthesis from 3-HAA, namely an ATP-dependent ligase and an amidohydrolase.[6] The two genes *natL2* and *natAM* from the nataxazole biosynthetic gene cluster of *Streptomyces* sp. Tü 6176, which code for the aforementioned enzymes, were inserted into a myxobacterial expression plasmid (Figure S3 in the Supporting Information).[17,18] After transferring the resulting vector pMEX14 into *M. xanthus* NM[19] and cultivation of the expression strain, LC–MS analysis of the bacterial raw extract indicated the presence of an amide shunt product (**1'a**)[6] as well as the benzoxazole product (**2a**; Figure 2). The identity of **2a** was confirmed by LC–MS/MS and NMR analyses, respectively (Figures S9 and S10).

With the benzoxazole-producing strain at our disposal, we further investigated the influence of substrate feeding on the titer of **2a** (Figure 3A). Without supplementation of any biosynthetic precursors, a product titer of 10.7 ± 1.8 mg L^{-1} was obtained in shake flasks. Feeding of 3-HAA to the *M. xanthus* cultures positively affected the production of **2a** in a concentration-dependent manner, although the molar yield coefficient decreased. This finding suggested that the amount of biocatalyst is a limiting factor under the given conditions or that substrate- or product-inhibitory effects occur. It is further noteworthy that the growth of *M. xanthus* NM: pMEX14 was inhibited with increasing amounts of 3-HAA (Figure 3B). In the presence of 480 mg L^{-1} 3-HAA, the growth was completely suppressed. The highest product titer (114.6 ± 7.4 mg L^{-1}) was achieved after the addition of 320 mg L^{-1} 3-HAA, with a yield coefficient of 40.6 ± 2.6 %.

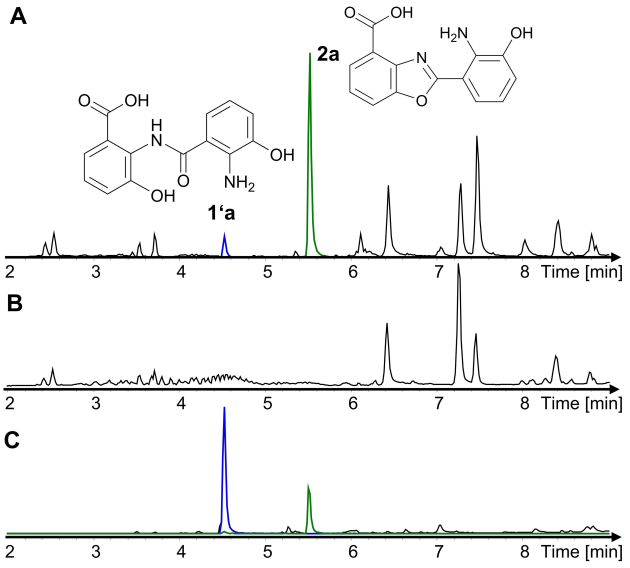

Figure 2. LC–MS chromatograms of A) the raw extract from *M. xanthus* NM: pMEX14, B) the plasmid-free *M. xanthus* NM control strain, and C) the in vitro reaction with isolated NatL2 and NatAM. Black: BPC, blue: EIC of **1'a** (*m/z* 289.0819), green: EIC of **2a** (*m/z* 271.0713).

As genomic analyses indicated that *M. xanthus* synthesizes 3-HAA from L-tryptophan via the kynurenine pathway, we also evaluated the effect of supplementing this amino acid to 1 mL cultures in a microbioreactor (Figure S13). While the growth of the myxobacterial host was only slightly affected, the production of **2a** increased with the concentration of L-tryptophan. Without feeding of the amino acid, a titer of 0.3 ± 0.1 mg L^{-1} was obtained. In presence of 1 g L^{-1} L-tryptophan, the production was roughly increased by a factor of 65 to 15.5 ± 1.7 mg L^{-1}. These values are significantly lower than the titers from the shake flask experiment, which probably is caused by the different cultivation condition and extraction method. To verify this assumption, we tested the effect of L-tryptophan supplementation in a shake flask experiment. When *M. xanthus* NM: pMEX14 was grown in the standard cultivation medium

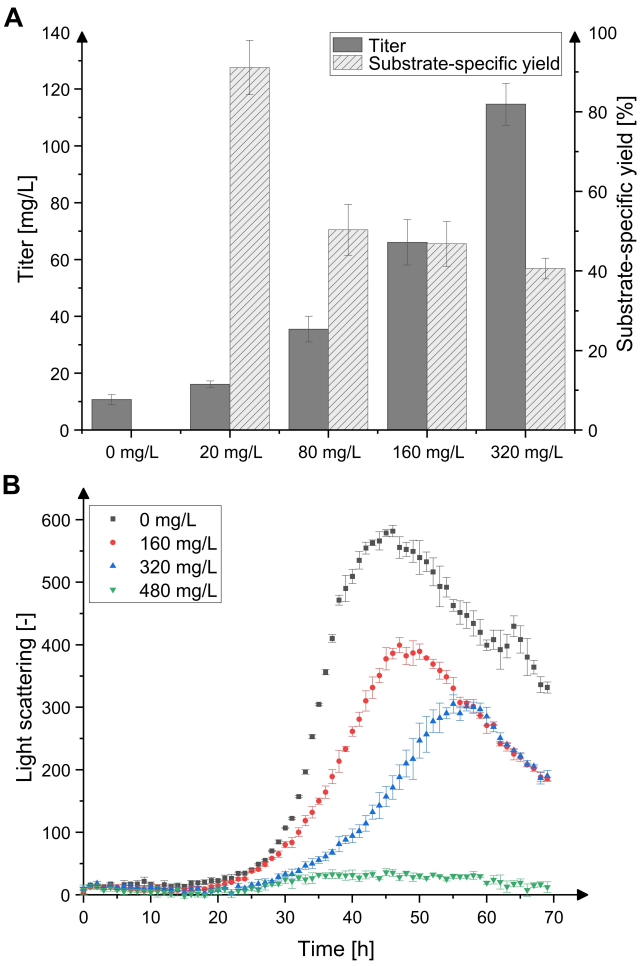

Figure 3. Influence of feeding *M. xanthus* NM: pMEX14 with 3-HAA. A) Production level of **2a** and molar substrate-specific yield. Product titers were determined after extraction of 50 mL cultures from shake flasks. B) Growth curves recorded in a microbioreactor system (BioLector, m2p-labs).

with addition of 1 g L^{-1} L-tryptophan, a product titer of 57.3 mg L^{-1} was observed.

Production of benzoxazoles in *E. coli* was only possible after feeding of 3-HAA and 6-methylsalicylic acid.[12] The highest product titers that were reported from recombinant *E. coli* cells are 3.5 mg L^{-1} in case of a methylated caboxamycin derivative and 4 mg L^{-1} in case of AJI9561 (Figure 1).[12] These titers were obtained following a two-day incubation, whereas the cultivation of *M. xanthus* took three days. However, care must be taken in the comparison of space-time yields (2 mg L^{-1} d^{-1} in *E. coli* and 38.2 mg L^{-1} d^{-1} in *M. xanthus*), as more benzoxazole biosynthesis genes were heterologously expressed in *E. coli*, which also led to a different product spectrum. Nevertheless, the present data indicate that *M. xanthus* is a promising host for recombinant benzoxazole production.

In vivo incorporation of endogenous and supplemented aromatic carboxylic acids into benzoxazoles

In the chemical analysis of *M. xanthus* NM: pMEX14, we consistently detected a low abundance peak (**2b**) that was not present in the plasmid-free control strain. The *m/z* value and the retention time of this peak suggested that it might belong to a structural analog of **2a**, but its low titer precluded an unequivocal structural identification. Foregoing studies had already indicated a possible crosstalk between benzoxazole biosynthesis and other natural product pathways. In particular, aromatic carboxylic acids, such as salicylic acid and 2,3-dihydroxybenzoic acid (2,3-DHBA), had been proposed to be diverted from siderophore pathways into benzoxazole biosynthesis.[7c,10,11] For that reason, we assumed that there might also be a crosstalk between the heterologously expressed benzoxazole biosynthesis enzymes and the native myxochelin pathway in *M. xanthus*, in which 2,3-DHBA represents an intermediate.[20] To test if 2,3-DHBA is indeed used by *M. xanthus* NM: pMEX14 for benzoxazole assembly, a culture of the expression strain was supplemented with additional 2,3-DHBA and its metabolic profile was recorded. In the corresponding chromatogram, the intensity of the previously observed low abundance peak (**2b**) was increased (Figure 4). LC–MS/MS suggested that **2b** represents a benzoxazole made from 3-HAA and 2,3-DHBA (Figure S14). Upon re-examination of the chromatogram a peak was detected, of which the $[M+H]^+$ ion is consistent with the amide shunt product **1'b**.

To assess the substrate tolerance of benzoxazole biosynthesis in *M. xanthus*, we fed our expression strain with other aryl carboxylic acids. Because an in vitro characterization of NatL2 and NatAM had indicated that these enzymes are capable of accepting 3-hydroxybenzoic acid (3-HBA) and its derivatives as substrates, we initially evaluated the combination of 3-HAA and 3-HBA.[6] After extraction of the bacterial culture, we detected the masses of the amides **1'a** and **1'c** as well as of the respective benzoxazoles **2a** and **2c** by LC–MS analysis

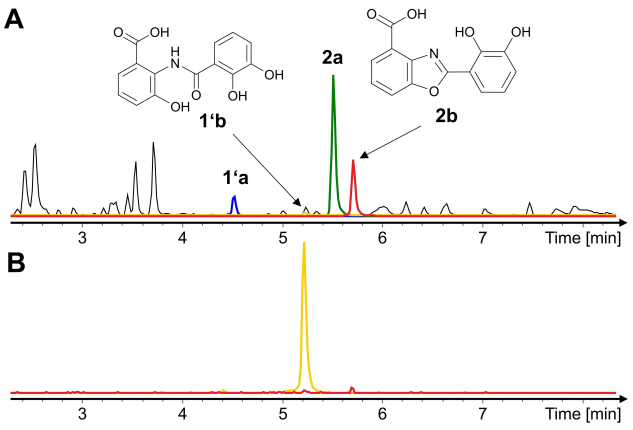

Figure 4. Incorporation of 2,3-DHBA into benzoxazoles. A) LC–MS chromatogram of the raw extract from *M. xanthus* NM: pMEX14 fed with 50 mg L^{-1} 3-HAA and 2,3-DHBA. B) In vitro reaction with isolated MxcE, NatL2 and NatAM. Blue: EIC of **1'a** (*m/z* 289.0819), green: EIC of **2a** (*m/z* 271.0713), yellow: EIC of **1'b** (*m/z* 290.0659), red: EIC of **2b** (*m/z* 272.0553).

(Figure S15). Interestingly, the signal corresponding to **2c** has a larger peak area than that of **2a**, indicating a preferred conversion. After HPLC purification, we obtained 1.3 mg of **1'c** and 2.1 mg of **2c** from a 50 mL culture. The structures of the two compounds were verified by NMR and MS analyses (Figures S16–S26). Subsequently, salicylic acid (SA), benzoic acid (BA) and 3-chlorobenzoic acid (3-ClBA) were successfully used as building blocks for the synthesis of benzoxazoles **2d-f** (Figures S27, S29, and S41). While **2d** corresponds to the known natural product caboxamycin,[7c] the BA- and 3-ClBA-derived benzoxazoles (**2e** and **2f**) have not been reported in the literature before. Compounds **1'e**, **2e**, **1'f** and **2f** were purified by HPLC. From 1 L cultures, we collected 18.8 mg of **1'e**, 3.4 mg of **2e**, 6.5 mg of **1'f** and 1.1 mg of **2f**. The purified derivatives were fully structurally characterized by spectroscopic analyses (Figures S30–S40 and S42–S52).

Involvement of a *M. xanthus* enzyme in combinatorial benzoxazole assembly

Next, we turned our attention to clarify the enzymatic basis of combinatorial benzoxazole assembly. Two scenarios were conceivable. Either the substrate flexibility of NatL2 and NatAM was sufficient to enable the synthesis of the benzoxazoles **2b**–**f** in *M. xanthus* depending on the availability of appropriate precursors or the participation of one or more host enzymes was additionally necessary. The question of which scenario applies to the observed crosstalk could not be answered on the basis of previous investigations.[6,7c,10,11]

In the second scenario, the *M. xanthus* enzyme MxcE was the most likely candidate for an involvement in benzoxazole assembly. In the biosynthesis of myxochelins, the ligase MxcE activates 2,3-DHBA as adenylate before its incorporation.[21] Moreover, MxcE is known to exhibit a broad substrate tolerance, which can be exploited for the biosynthesis of myxochelin analogs incorporating different aryl carboxylic acids.[22] We thus hypothesized that MxcE had possibly contributed to the outcome of our feeding experiments. In order to probe this possibility, an in vitro testing of the aforementioned enzymes was carried out. For this, we expressed *natL2* and *natAM* as well as *mxcE* in *E. coli* BL21(DE3) as hexahistidyl-tagged recombinant proteins using pET28a(+)-derived plasmids. The enzymes were purified via Ni-NTA affinity chromatography. Subsequently, in vitro reactions were performed with different enzyme combinations using 0.5 mM 3-HAA and 0.5 mM of another aryl carboxylic acid (2,3-DHBA, 3-HBA, SA, BA, or 3-ClBA) as substrates. The exclusive combination of MxcE and NatAM did not lead to any product formation in absence of NatL2. This shows that MxcE is not able to entirely substitute the activity of NatL2. Subsequently, we compared the product profiles from reactions including the enzymes MxcE, NatL2 and NatAM with those of NatL2 and NatAM only (Table 1). In presence of MxcE, the areas of all detected amide and product peaks were increased. As expected from a previous study,[6] only NatL2 and NatAM were needed for the in vitro synthesis of the 3-HBA-derived benzoxazole (**2c**). Still, the presence of MxcE improved the production level of **2c** by 46% (Table S3). While it was not possible to produce the 2,3-DHBA- and SA-derived benzoxazoles in reactions with NatL2 and NatAM alone, the addition of MxcE allowed the synthesis of both 3-hydroxycaboxamycin (**2b**) and caboxamycin (**2d**). The BA- and 3-ClBA-derived benzoxazoles (**2e**, **2f**) could not be generated in vitro. Although the addition of MxcE positively affected the production of **1'e** and **1'f**, which can be expected to derive from the relevant ester intermediates **1e** and **1f**, no heterocyclization was observed. We assume that this is due to comparatively low titers of **1e** and **1f**. The NatAM reaction is likely not favored in an aqueous phase for thermodynamic reasons. Higher concentrations of the ester intermediate would thus be necessary to promote benzoxazole formation. This is also supported by the formation of **2b** after addition of MxcE (Table 1). In case of **1e** and **1f**, it cannot be excluded that they occur in higher concentrations in vivo, as *M. xanthus* enzymes other than MxcE could also contribute to the activation of their building blocks.

Consolidating our results with observations made by other groups, it is now possible to deduce a model for the combinatorial biosynthesis of benzoxazoles in *M. xanthus* and in other bacteria (Figure 5).[6,7c,10,11] According to this model, a NatL2-type enzyme is essential for benzoxazole formation,

Table 1. Benzoxazoles produced by in vitro biotransformation of two substrates with NatL2 and NatAM in the absence or presence of MxcE.

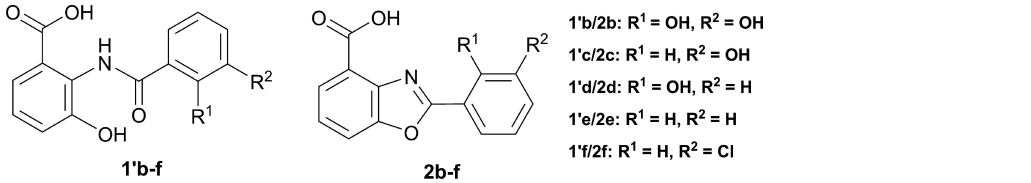

Substrate #1	Substrate #2	Amide shunt product	Peak area of amide shunt product in relation to **1'a** [%] after reaction w/o MxcE	after reaction with MxcE	Benzoxazole product	Peak area of benzoxazole product in relation to **2a** [%] after reaction w/o MxcE	after reaction with MxcE
3-HAA	2,3-DHBA	**1'b**	8.7%	9.6%	**2b**	0.0%	0.1%
3-HAA	3-HBA	**1'c**	24.3%	24.0%	**2c**	25.5%	26.4%
3-HAA	SA	**1'd**	0.0%	0.4%	**2d**	0.0%	1.6%
3-HAA	BA	**1'e**	0.2%	0.4%	**2e**	0.0%	0.0%
3-HAA	3-ClBA	**1'f**	0.3%	0.3%	**2f**	0.0%	0.0%

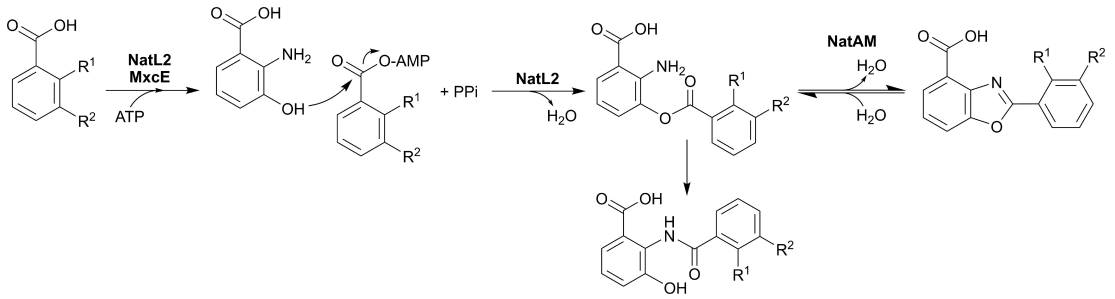

Figure 5. Proposed reaction mechanism for benzoxazole biosynthesis in *M. xanthus* including spontaneous conversion of the ester intermediate into an amide shunt product. The *mxcE* gene is naturally present in the chromosome of *M. xanthus*, whereas the genes *natL2* and *natAM* originate from *Streptomyces* sp. Tü 6176 and were heterologously expressed in *M. xanthus*.

because of its ability to link 3-HAA with other aryl carboxylic acid adenylates. When it comes to the adenylation reaction, however, there is some redundancy, in that other enzymes can activate utilizable building blocks in a manner similar to NatL2. Such enzymes (e.g., MxcE) might even expand the product spectrum depending on their substrate tolerance. It is thus evident that benzoxazole biosynthesis not only draws metabolites from other pathways, but that it also capitalizes on ligases of other pathways. This finding has important implications for the biotechnological production of benzoxazoles. In brief, the heterocyclic scaffold can be furnished with different substituents by combining benzoxazole biosynthesis pathways with other adenylating enzymes.[23] The 4-halobenzoate-coenzyme A ligase from *Pseudomonas* sp. CBS-3 or the naphthoic acid-coenzyme A ligase NcsB2 from *Streptomyces carzinostaticus* ATCC15944 are examples of characterized adenylation enzymes that exhibit a broad substrate specificity.[24] Other alternatives might be found in adenylation domains of nonribosomal peptide synthetases that can be engineered for modification of the substrate specificity, as exemplified by the DhbE adenylation domain from enterobactin biosynthesis.[25] One must take into account, however, that the substrate tolerance of the heterocycle-forming amidohydrolase NatAM might become a limiting factor for the combinatorial biosynthesis of benzoxazoles, which should be further investigated in future.

Conclusions

Beside synthetic approaches for derivatization, concepts of bioengineering that include semisynthesis, combinatorial biosynthesis, precursor-directed biosynthesis, mutasynthesis or in vitro biocatalysis have been established for natural product derivatization over the past decades.[26] In this study, we evaluated *M. xanthus* as an alternative host organism for the generation of benzoxazole-containing natural products. The myxobacterium *M. xanthus* naturally produces the required building block 3-hydroxyanthranilic acid (3-HAA), facilitating the synthesis of benzoxazoles upon heterologous expression of only two genes from the nataxazole biosynthetic pathway. Additional supplementation of 3-HAA led to competitive space–time yields in *M. xanthus* of up to 38 $mg\,L^{-1}\,d^{-1}$. This exceeds the yield previously reported from *E. coli* (2 $mg\,L^{-1}\,d^{-1}$), which is not able to produce benzoxazoles without the addition of 3-HAA.[12] However, care must be taken in the comparison of these values, as the reconstruction of benzoxazole biosynthesis in *E. coli* involved the heterologous expression of a total of five genes, which also led to a different product spectrum.

In *M. xanthus*, various benzoic acid-derived building blocks activated by the adenylating enzyme MxcE can be incorporated into the benzoxazole scaffold, representing crosstalk between the native myxochelin pathway and the heterologously expressed benzoxazole pathway. This biocombinatorial concept opens new opportunities for the assembly of benzoxazole analogs, considering the large diversity of adenylating enzymes in natural product pathways. In the future, it will be interesting to evaluate the production of structurally more complex benzoxazoles in *M. xanthus* and also to tune the expression of the biosynthesis genes in order to further increase the product titers. Promoter engineering would be one promising approach for the latter task.[27]

Experimental Section

Strains, nucleic acids, and plasmids: The bacterial strains and plasmids used in this study are described in Table S1. The nonmotile strain *M. xanthus* NM[19] was purchased from the American Type Culture Collection (ATCC). The genes *natL2* and *natAM* originating from the nataxazole gene cluster (GenBank accession number LN713864) were codon-optimized for *M. xanthus* and subsequently synthesized by Life Technologies GmbH (Thermo Fisher Scientific, see Supporting Information). For *E. coli*, the codon-optimized genes published by Ouyang et al. were used.[12]

Growth conditions and nucleic acid extraction: *E. coli* TOP10 was cultured in liquid or solidified lysogeny broth (LB) medium at 37 °C. Liquid cultures were shaken at 180 rpm. *M. xanthus* was grown in CYE medium (10 $g\,L^{-1}$ casitone, 5 $g\,L^{-1}$ yeast extract, 2.1 $g\,L^{-1}$ MOPS, 1 $g\,L^{-1}$ $MgSO_4{\cdot}7H_2O$, 0.5 $mg\,L^{-1}$ vitamin B12; pH 7.4) at 30 °C. For liquid cultures, an agitation speed of 130 rpm was applied. The antibiotic kanamycin (50 $\mu g\,L^{-1}$) was used as selection marker. Plasmid DNA was obtained from *E. coli* cultures using the NucleoSpin Plasmid (NoLid) Mini Kit (Macherey-Nagel). Nucleic acids embedded in agarose gels were isolated using the NucleoSpin Gel and PCR Clean-up Mini Kit (Macherey-Nagel).

General cloning procedure: Plasmid construction was generally performed by making use of the Gibson assembly method.[28] For this purpose, the insert DNA fragments were amplified by overhang PCR using the Phusion High-Fidelity DNA polymerase (ThermoScientific). Circular plasmid DNA was linearized with FastDigest restriction enzymes (ThermoScientific) and dephosphorylated with the FastAP alkaline phosphatase (ThermoScientific) to avoid recircularization. For DNA assembly, 2x GeneArt Gibson Assembly HiFi Master Mix (Invitrogen) was mixed with 50 ng linear plasmid DNA in a reaction volume of 10 μL. The amount of insert DNA was adjusted to different insert/vector ratios (1:1, 3:1, 5:1). The reaction mixture was incubated for 60 min at 50 °C. Subsequently, the assembled plasmids were introduced into chemically competent *E. coli* TOP10 cells.

Construction of *M. xanthus* NM: pMEX14: The *E. coli-M. xanthus* shuttle vector pMEX03[17] carrying the *pilA*-promoter (P_{pilA}) and the first 15 codon of the *pilA*-gene was linearized using the restriction enzyme ScaI. The synthetically prepared genes *natL2* and *natAM* were amplified with the primer pairs P01/P02 or P03/P04 (Table S2) to add Gibson overhangs. Both genes were cloned into the ScaI-restriction site of the linearized pMEX03 via Gibson assembly to create the vectors pMEX12 and pMEX13 (Figures S1 and S2). Subsequently, the construct P_{pilA}-*natAM* was amplified with the primers P05/P06 and integrated into the ScaI-site of pMEX12 to give the expression plasmid pMEX14 (Figure S3). All plasmids were transferred into chemically competent *E. coli* TOP10 cells and validated via colony PCR (primer pair P07/P08) and sequencing. The plasmid pMEX14 was introduced into electrocompetent *M. xanthus* NM cells according to a previously published protocol.[16] Successful plasmid uptake was confirmed by colony PCR using the primer pairs P09/P10 and P08/P11, respectively (Figure S4).

Production of benzoxazoles in *M. xanthus*: Well grown seed cultures of *M. xanthus* NM: pMEX14 were inoculated into 50 mL CYE medium with 50 μg mL^{-1} kanamycin to an $OD_{600\,nm}$ of 0.05. For the production of **2a**, 20 mg L^{-1} 3-HAA were added as a supplement. For the generation of **2b**–**f**, the cultures were individually fed with 50 mg L^{-1} 3-HAA and 50 mg L^{-1} of another aryl carboxylic acid (2,3-DHBA, 3-HBA, SA, BA or 3-ClBA). After three days of incubation at 30 °C and 130 rpm, 3% (*w/v*) of the adsorber resin Amberlite XAD7HP (Sigma–Aldrich) were added, and the cultures were incubated for two additional hours. Afterwards, the adsorber resin was collected by filtration and washed with 100 mL water. Elution of adsorbed compounds was performed by adding 100 mL methanol. The bacterial raw extract was concentrated using a rotary evaporator (Heidolph) and analyzed via LC–MS. For isolation of the compounds **1'e** and **2e**, and **1'f** and **2f**, the cultivation was repeated and upscaled to a volume of 1 L CYE medium. The compounds **1'c** and **2c**, **1'e** and **2e**, and **1'f** and **2f** were purified via HPLC (Shimadzu) by applying the following chromatographic conditions: Flow rate: 4 mL/min. Mobile phases: acetonitrile (ACN) and water with 0.1% (*v/v*) trifluoroacetic acid. Column: VP250/10 Nucleodur C_{18} Isis, 5 μm (Macherey-Nagel). Gradient: 0–5 min: 30% ACN; 5–20 min: 30–50% ACN; 20–25 min: 50–100% ACN; 25–27 min: 100% ACN; 27–28 min: 100–30% ACN; 28–32 min: 30% ACN. Retention times: **1'c**–14 min; **2c**–15 min; **1'e**–19.2 min; **2e**–21 min; **1'f**–23.8 min; **2f**–24.5 min.

Quantification of 2a produced by *M. xanthus*: For preparative isolation of **2a**, *M. xanthus* NM: pMEX14 was cultured in 100 mL CYE medium supplemented with 50 μg mL^{-1} kanamycin and 20 mg L^{-1} 3-HAA. Product isolation and purification was conducted as described above. The retention time of **2a** was 17.2 min under the chosen HPLC conditions. After purification, compound **2a** was subjected to NMR analysis (Figure S10). To quantify the amount of **2a** in bacterial raw extracts, a calibration curve between the UV peak area at 320 nm and the injected mass of **2a** was recorded (Figure S11). The following HPLC conditions were applied for product quantification: Flow rate: 1 mL/min. Mobile phases: acetonitrile and water with 0.1% (*v/v*) trifluoroacetic acid. Column: EC 250/4 Nucleodur C_{18} Isis, 5 μm (Macherey–Nagel). Column oven: 30 °C. Gradient: 0–5 min: 30% ACN; 5–16 min: 30–81% ACN; 16–18 min 81–100% ACN; 18–20 min: 100% ACN; 20–21 min: 100–30% ACN; 21–25 min: 30% ACN. Retention time of **2a**: 12.6 min.

Feeding experiments: Growth curves of *M. xanthus* NM: pMEX14 were recorded using the microbioreactor BioLector I (m2p-labs) and 48 well flower-shaped microtiter plates (FlowerPlates, m2p-labs). A defined volume of CYE medium containing kanamycin (50 μg mL^{-1}) was inoculated with a seed culture to an $OD_{600\,nm}$ of 0.1. Each well was filled with 990 μL of this cell suspension or with sterile CYE medium, alternatively. 10 μL of 3-HAA or L-tryptophan stock solutions (60% (*v/v*) DMSO) were added. The microcultures were incubated at 30 °C, 1000 rpm and a humidity of 85%. The light scattering was measured every hour. Each experiment was conducted in triplicate. If necessary, the cultures from the BioLector experiments were transferred to 2 mL-Eppendorf tubes and extracted two times with ethyl acetate. The ethyl acetate was evaporated in a vacuum concentrator (Concentrator plus, Eppendorf) and the dried extract was dissolved in 100 μL methanol for HPLC-UV analysis. Additionally, the 3-HAA feeding experiment was repeated in shake flasks. For this, 50 mL CYE medium containing 50 μg mL^{-1} kanamycin were inoculated with a preculture of *M. xanthus* NM: pMEX14 to an $OD_{600\,nm}$ of 0.05. The cultures were supplemented with 0, 20, 80, 160 and 320 mg L^{-1} 3-HAA and incubated for 3 days at 30 °C and 130 rpm. Product isolation was performed with the adsorber resin Amberlite XAD7HP as described above. Each experiment was performed in three replicates.

Spectroscopic analyses: LC–MS measurements were conducted in positive mode using an Agilent 1260 Infinity HPLC system combined with a Bruker Daltonics Compact quadrupole time of flight mass spectrometer. The HPLC was operated with Nucleoshell RP 18 ec column (100×2 mm, 2.7 μm; Macherey–Nagel) at the following conditions: Flow rate: 0.4 mL/min. Column oven: 40 °C. Mobile phases: acetonitrile and water with 0.1% (*v/v*) formic acid. Gradient: 0–10 min: 2–98% ACN; 10–15 min: 98% ACN; 15–17 min: 98–5% ACN; 17–20 min: 5% ACN; 27–28 min: 100–30% ACN; 28–32 min: 30% ACN. The MS analyses were performed at a capillary voltage of 4.5 kV, a desolvation gas (N_2) temperature of 220 °C and a dry gas (N_2) flow rate of 12 L/min. LC–MS/MS measurements were performed with collision energies of 18, 23 or 30 eV. NMR measurements were carried out at ambient temperature using a Bruker AV 700 Avance III HD (CryoProbe) spectrometer, which is equipped with a 5 mm helium-cooled inverse quadrupol resonance cryoprobe. The NMR spectra were recorded with deuterated chloroform ($CDCl_3$) or methanol (MeOD) as solvent and internal standard (chloroform-*d*: δ_H 7.24 ppm and δ_C 77.0 ppm; methanol-d_4: δ_H 3.31 ppm and δ_C 49.0 ppm).

2-(2,3-Dihydroxybenzamido)-3-hydroxybenzoic acid (**1'c**): ^{1}H NMR (700 MHz, MeOD, 300 K): $\delta = 7.66$ (dd, $J = 7.5$, 1.8 Hz, 1H, CH-6), 7.54 (ddd, $J = 7.7$, 1.8, 0.9 Hz, 1H, CH-13), 7.48 (dd, $J = 2.5$, 1.8 Hz, 1H, CH-9), 7.36 (t, $J = 8.0$, 7.8 Hz, 1H, CH-12), 7.21 (t, $J = 8.3$, 7.5 Hz, 1H, CH-5), 7.18 (dd, $J = 8.3$, 1.8 Hz, 1H, CH-4), 7.04 (ddd, $J = 8.1$, 2.5, 0.9 Hz, 1H, CH-11); ^{13}C NMR (175 MHz, MeOD, 300 K): $\delta = 172.0$ (C-7), 169.0 (C-14), 159.2 (C-10), 151.6 (C-3), 135.9 (C-8), 131.0 (C-12), 129.0 (C-2), 127.1 (C-5), 124.7 (C-4), 124.4 (C-1), 124.2 (C-6), 120.7 (C-11), 119.8 (C-13), 115.8 (C-9); HRMS (ESI): *m/z* calcd for $C_{14}H_{11}NO_5$: 274.0710 [$M + H$]$^+$; found: 274.0703.

2-Benzamido-3-hydroxybenzoic acid (**1'e**): ^{1}H NMR (700 MHz, MeOD, 300 K): $\delta = 8.07$ (dd, $J = 8.3$, 1.3 Hz, 2H, CH-9, CH-13), 7.66 (dd, $J = 7.2$, 2.2 Hz, 1H, CH-6), 7.63 (dt, $J = 7.5$, 1.3 Hz, 1H, CH-11), 7.55 (t, $J = 8.3$, 7.5 Hz, 2H, CH-10, CH-12), 7.22 (t, $J = 8.0$, 7.2 Hz, 1H,

CH-5), 7.21 (dd, $J=8.0$, 2.2 Hz, 1H, CH-4); ^{13}C NMR (175 MHz, MeOD, 300 K): $\delta=171.4$ (C-7), 169.0 (C-14), 151.9 (C-3), 134.5 (C-8), 133.7 (C-11), 129.9 (C-10), 129.9 (C-12), 128.9 (C-9), 128.9 (C-13), 128.8 (C-2), 127.4 (C-5), 124.9 (C-4), 124.2 (C-6), 123.9 (C-1); HRMS (ESI): *m/z* calcd for $C_{14}H_{11}NO_4$: 258.0761 $[M+H]^+$; found: 258.0772.

2-(3-Chlorobenzamido)-3-hydroxybenzoic acid (**1'f**): ^1H NMR (700 MHz, MeOD, 300 K): $\delta=8.06$ (s, 1H, CH-9), 7.99 (d, $J=8.0$ Hz, 1H, CH-13), 7.64 (dd, $J=8.0$, 1.5 Hz, 1H, CH-6), 7.63 (d, $J=7.9$ Hz, 1H, CH-11), 7.54 (t, $J=7.9$ Hz, 1H, CH-12), 7.24 (t, $J=8.0$ Hz, 1H, CH-5), 7.20 (dd, $J=8.0$, 1.5 Hz, 1H, CH-4); ^{13}C NMR (175 MHz, MeOD, 300 K): $\delta=171.1$ (C-7), 167.6 (C-14), 152.4 (C-3), 136.8 (C-10), 135.9 (C-8), 133.4 (C-11), 131.5 (C-12), 129.1 (C-9), 128.0 (C-2), 127.7 (C-5), 127.2 (C-13), 125.1 (C-1), 124.3 (C-4), 124.0 (C-6); HRMS (ESI): *m/z* calcd for $C_{14}H_{10}ClNO_4$: 292.0371 $[M+H]^+$; found: 292.0372.

2-(2,3-Dihydroxyphenyl)benzo[*d*]oxazole-4-carboxylic acid (**2c**): ^1H NMR (700 MHz, MeOD, 300 K): $\delta=8.04$ (dd, $J=7.8$, 1.0 Hz, 1H, CH-6), 7.92 (dd, $J=8.0$, 1.0 Hz, 1H, CH-4), 7.83 (ddd, $J=7.7$, 1.8, 0.9 Hz, 1H, CH-13), 7.76 (dd, $J=2.5$, 1.8 Hz, 1H, CH-9), 7.51 (t, $J=7.9$ Hz, 1H, CH-5), 7.41 (t, $J=7.9$ Hz, 1H, CH-12), 7.05 (ddd, $J=8.1$, 2.5, 0.9 Hz, 1H, CH-11); ^{13}C NMR (175 MHz, MeOD, 300 K): $\delta=168.0$ (C-7), 166.2 (C-14), 159.3 (C-10), 152.7 (C-3), 142.7 (C-2), 131.4 (C-12), 128.7 (C-8), 128.3 (C-6), 126.0 (C-5), 123.4 (C-1), 120.7 (C-11), 120.4 (C-13), 116.2 (C-4), 115.6 (C-9); HRMS (ESI): *m/z* calcd for $C_{14}H_9NO_4$: 256.0604 $[M+H]^+$; found: 256.0602.

2-Phenylbenzo[*d*]oxazole-4-carboxylic acid (**2e**): ^1H NMR (700 MHz, MeOD, 300 K): $\delta=8.37$ (dd, $J=7.0$, 1.6 Hz, 2H, CH-9, CH-13), 8.04 (dd, $J=7.7$, 1.1 Hz, 1H, CH-6), 7.94 (dd, $J=8.1$, 1.1 Hz, 1H, CH-4), 7.63 (m, 1H, CH-11), 7.60 (t, $J=7.6$, 7.0 Hz, 2H, CH-10, CH-12), 7.52 (t, $J=7.9$ Hz, 1H, CH-5); ^{13}C NMR (175 MHz, MeOD, 300 K): $\delta=168.0$ (C-7), 166.1 (C-14), 152.7 (C-3), 142.7 (C-2), 133.5 (C-11), 130.2 (C-10), 130.2 (C-12), 129.2 (C-9), 129.2 (C-13), 128.3 (C-6), 127.7 (C-8), 126.0 (C-5), 123.4 (C-1), 116.2 (C-4); HRMS (ESI): *m/z* calcd for $C_{14}H_9NO_3$: 240.0655 $[M+H]^+$; found: 240.0668.

2-(3-Chlorophenyl)benzo[*d*]oxazole-4-carboxylic acid (**2f**): ^1H NMR (700 MHz, $CDCl_3$, 300 K): $\delta=8.27$ (s, 1H, CH-9), 8.18 (d, $J=7.7$ Hz, 1H, CH-13), 8.18 (d, $J=7.9$ Hz, 1H, CH-6), 7.83 (d, $J=7.9$ Hz, 1H, CH-4), 7.60 (d, $J=7.7$ Hz, 1H, CH-11), 7.54 (t, $J=7.9$ Hz, 1H, CH-5), 7.52 (t, $J=7.7$ Hz, 1H, CH-12),; ^{13}C NMR (175 MHz, $CDCl_3$, 300 K): $\delta=164.3$ (C-7), 163.1 (C-14), 150.4 (C-3), 140.6 (C-2), 135.5 (C-10), 133.1 (C-11), 130.6 (C-12), 128.2 (C-9), 127.8 (C-6), 127.0 (C-8), 126.3 (C-13), 126.1 (C-5), 120.4 (C-1), 115.6 (C-4); HRMS (ESI): *m/z* calcd for $C_{14}H_8ClNO_3$: 274.0265 $[M+H]^+$; found: 274.0267.

Construction of expression plasmids for NatL2, NatAM and MxcE: For in vitro analysis, the enzymes NatL2, NatAM and MxcE were produced as His-tagged enzymes in *E. coli*. For that purpose, the respective genes were amplified with the primer pairs P12/P13 (*natL2*), P14/P15 (*natAM*), and P16/P17 (*mxcE*) to attach Gibson overhangs. Afterwards, the PCR products were cloned into the Eco53kI restriction site of the plasmid pET28a(+) via Gibson assembly. The identity of the plasmids pET28a(+)-*natL2*, pET28a(+)-*natAM*, pET28a(+)-*mxcE* was confirmed via colony PCR (primers P18/P19) and Sanger sequencing (Figures S5–S7). The validated plasmids were introduced into *E. coli* BL21(DE3) by chemical transformation.

Enzyme production and purification: The expression strains were cultivated in terrific broth (12 g L^{-1} tryptone/peptone, 24 g L^{-1} yeast extract, 4 mL/L glycerol, 2.3 g L^{-1} KH_2PO_4, 12.5 g L^{-1} K_2HPO_4) at 37 °C until an $OD_{600\,nm}$ of 0.6 was reached. Then, the T7 expression system was induced by addition of 1 mM isopropyl-β-D-1-thiogalactopyranoside (IPTG) and incubated for 20 h at 16 °C. The cells were harvested by centrifugation (ThermoScientific Heraeus Multifuge 1S-R, rotor TTH400, 4500 rpm, 15 min, 4 °C) and resuspended in lysis buffer (50 mM NaH_2PO_4, 10 mM imidazole, 300 mM NaCl, 100 mL/L glycerol, pH 8). The cells were lysed by ultrasonication (5 cycles of 30 s, 4 °C, 10% amplitude) and the cell debris was removed via centrifugation (ThermoScientific Sorvall RC6+ centrifuge, rotor F13-14x50cy, 13000 rpm, 20 min, 4 °C). The supernatant was subjected to Ni-nitrilotriacetic acid (NiNTA) affinity chromatography. For this, 2 mL Protino NiNTA agarose (Macherey–Nagel) were transferred into a polypropylene column and equilibrated with 10 mL lysis buffer. Afterwards, the supernatant containing the His-tagged enzymes was applied. For removal of contaminating proteins, the matrix was washed with 5 mL washing buffer I (lysis buffer containing 20 mM imidazole) and 5 mL washing buffer II (lysis buffer containing 40 mM imidazole). Protein elution was performed by adding 2.5 mL elution buffer (lysis buffer containing 250 mM imidazole). The enzyme solutions were desalted using PD-10 desalting columns (Cytiva) according to the manufacturer's specification. For column equilibration, 100 mM Tris·NaCl buffer (20 mM Tris, 100 mM NaCl, 100 mL/L glycerol, pH 8) was used. The enzyme solutions were analyzed by SDS PAGE (Figure S8) and the protein concentration was measured with the UV-Vis spectrometer NanoDrop One (Thermo Fisher Scientific) at 280 nm.

In vitro assays: Enzymatic reactions were generally conducted in 50 mM Tris·HCl buffer (pH 8) with 0.7 μM of each enzyme, 1 mM ATP and 10 mM $MgCl_2$ in a total volume of 200 μL. For in vitro synthesis of compounds **1'a** and **2a**, 1 mM 3-HAA was used as substrate. For synthesis of the derivatives **1'b**–**f** and **2b**–**f**, 0.5 mM 3-HAA and 0.5 mM of the respective benzoic acid-derived building block were added. Three different combinations of enzymes were tested: i) MxcE and NatAM, ii) MxcE, NatL2 and NatAM, and iii) NatL2 and NatAM. All reactions were incubated for 20 h at 30 °C and 400 rpm in a thermomixer (Eppendorf). The reactions were stopped by addition of 1 V methanol and analyzed by LC–MS.

Acknowledgements

Financial support from the European Regional Development Fund (grant EFRE-0300098 to M.N.) is gratefully acknowledged. We further thank Professors Stephan Lütz and Oliver Kayser (both TU Dortmund University) for providing access to their LC/MS facilities. Open Access funding enabled and organized by Projekt DEAL.

Conflict of Interest

The authors declare no conflict of interest.

Data Availability Statement

The data that support the findings of this study are available in the supplementary material of this article.

Keywords: benzoxazole · combinatorial biosynthesis · heterologous expression · ligases · *Myxococcus xanthus*

[1] C. Lamberth, J. Dinges, *Bioactive Heterocyclic Compound Classes. Pharmaceuticals*, Wiley-VCH, Weinheim, **2012**.
[2] a) K. Martina, S. Tagliapietra, V. V. Veselov, G. Cravotto, *Front. Chem.* **2019**, *7*, 95; b) M. V. Murlykina, A. D. Morozova, I. M. Zviagin, Y. I. Sakhno, S. M. Desenko, V. A. Chebanov, *Front. Chem.* **2018**, *6*, 527; c) M. Henary, C. Kananda, L. Rotolo, B. Savino, E. A. Owens, G. Cravotto, *RSC*

Adv. **2020**, *10*, 14170–14197; d) M. Maji, D. Panja, I. Borthakur, S. Kundu, *Org. Chem. Front.* **2021**, *8*, 2673–2709; e) W. Guo, M. Zhao, W. Tan, L. Zheng, K. Tao, X. Fan, *Org. Chem. Front.* **2019**, *6*, 2120–2141.
[3] a) F. Hemmerling, F. Hahn, *Beilstein J. Org. Chem.* **2016**, *12*, 1512–1550; b) B. Gao, B. Yang, X. Feng, C. Li, *Nat. Prod. Rep.* **2022**, *39*, 139–162.
[4] L. Winand, D. J. Vollmann, J. Hentschel, M. Nett, *Catalysts* **2021**, *11*, 892.
[5] J. Korp, L. Winand, A. Sester, M. Nett, *Appl. Environ. Microbiol.* **2018**, *84*, e01789-18.
[6] H. Song, C. Rao, Z. Deng, Y. Yu, J. H. Naismith, *Angew. Chem. Int. Ed.* **2020**, *59*, 6054–6061; *Angew. Chem.* **2020**, *132*, 6110–6117.
[7] a) C. Cano-Prieto, R. García-Salcedo, M. Sánchez-Hidalgo, A. F. Braña, H.-P. Fiedler, C. Méndez, J. A. Salas, C. Olano, *ChemBioChem* **2015**, *16*, 1461–1473; b) M. Lv, J. Zhao, Z. Deng, Y. Yu, *Chem. Biol.* **2015**, *22*, 1313–1324; c) A. A. Losada, C. Cano-Prieto, R. García-Salcedo, A. F. Braña, C. Méndez, J. A. Salas, C. Olano, *Microb. Biotechnol.* **2017**, *10*, 873–885; d) C. Hohmann, K. Schneider, C. Bruntner, E. Irran, G. Nicholson, A. T. Bull, A. L. Jones, R. Brown, J. E. M. Stach, M. Goodfellow, *J. Antibiot.* **2009**, *62*, 99–104.
[8] T. Horch, E. M. Molloy, F. Bredy, V. G. Haensch, K. Scherlach, K. L. Dunbar, J. Franke, C. Hertweck, *Angew. Chem. Int. Ed.* **2022**, *61*, e202205409.
[9] a) X. K. Wong, K. Y. Yeong, *ChemMedChem* **2021**, *16*, 3237–3262; b) L. P. H. Yang, *Drugs* **2014**, *74*, 1817–1822; c) J. Park, U. Egolum, S. Parker, E. Andrews, D. Ombengi, H. Ling, *Ann. Pharmacother.* **2020**, *54*, 470–477; d) D.-L. Dong, Y. Luan, T.-M. Feng, C.-L. Fan, P. Yue, Z.-J. Sun, R.-M. Gu, B.-F. Yang, *Eur. J. Pharmacol.* **2006**, *545*, 161–166.
[10] C. Cano-Prieto, A. A. Losada, A. F. Braña, C. Méndez, J. A. Salas, C. Olano, *ChemBioChem* **2015**, *16*, 1925–1932.
[11] A. A. Losada, C. Méndez, J. A. Salas, C. Olano, *Microb. Cell Fact.* **2017**, *16*, 93.
[12] H. Ouyang, J. Hong, J. Malroy, X. Zhu, *ACS Synth. Biol.* **2021**, *10*, 2151–2158.
[13] M. Kanehisa, S. Goto, *Nucleic Acids Res.* **2000**, *28*, 27–30.
[14] a) D. Pogorevc, F. Panter, C. Schillinger, R. Jansen, S. C. Wenzel, R. Müller, *Metab. Eng.* **2019**, *55*, 201–211; b) D. Pogorevc, Y. Tang, M. Hoffmann, G. Zipf, H. S. Bernauer, A. Popoff, H. Steinmetz, S. C. Wenzel, *ACS Synth. Biol.* **2019**, *8*, 1121–1133.
[15] a) C. Oßwald, G. Zipf, G. Schmidt, J. Maier, H. S. Bernauer, R. Müller, S. C. Wenzel, *ACS Synth. Biol.* **2014**, *3*, 759–772; b) D. C. Stevens, M. R. Henry, K. A. Murphy, C. N. Boddy, *Appl. Environ. Microbiol.* **2010**, *76*, 2681–2683; c) D. C. Stevens, K. R. Conway, N. Pearce, L. Roberto Villegas-Peñaranda, A. G. Garza, C. N. Boddy, *PLoS One* **2013**, *8*, e64858.
[16] B. K. Lombe, L. Winand, J. Diettrich, M. Töbermann, W. Hiller, M. Kaiser, M. Nett, *Org. Lett.* **2022**, *24*, 2935–2939.
[17] L. Winand, P. Schneider, S. Kruth, N.-J. Greven, W. Hiller, M. Kaiser, J. Pietruszka, M. Nett, *Org. Lett.* **2021**, *23*, 6563–6567.
[18] J.-Y. Zhao, L. Zhong, M.-J. Shen, Z.-J. Xia, Q.-X. Cheng, X. Sun, G.-P. Zhao, Y.-Z. Li, Z.-J. Qin, *Appl. Environ. Microbiol.* **2008**, *74*, 1980–1987.
[19] R. P. Burchard, *J. Bacteriol.* **1970**, *104*, 940–947.
[20] B. Silakowski, B. Kunze, G. Nordsiek, H. Blöcker, G. Höfle, R. Müller, *Eur. J. Biochem.* **2000**, *267*, 6476–6485.
[21] N. Gaitatzis, B. Kunze, R. Müller, *Proc. Natl. Acad. Sci. USA* **2001**, *98*, 11136–11141.
[22] a) N. A. Frank, M. Széles, S. H. Akone, S. Rasheed, S. Hüttel, S. Frewert, M. M. Hamed, J. Herrmann, S. M. M. Schuler, A. K. H. Hirsch, R. Müller, *Molecules* **2021**, *26*, 4929; b) D.-G. Wang, L. Niu, Z.-M. Lin, J.-J. Wang, D.-F. Gao, H.-Y. Sui, Y.-Z. Li, C. Wu, *J. Nat. Prod.* **2021**, *84*, 2744–2748; c) A. Sester, L. Winand, S. Pace, W. Hiller, O. Werz, M. Nett, *J. Nat. Prod.* **2019**, *82*, 2544–2549; d) J. Korp, S. König, S. Schieferdecker, H.-M. Dahse, G. M. König, O. Werz, M. Nett, *ChemBioChem* **2015**, *16*, 2445–2450.
[23] H. K. D'Ambrosio, E. R. Derbyshire, *ACS Chem. Biol.* **2020**, *15*, 17–27.
[24] a) H. A. Cooke, J. Zhang, M. A. Griffin, K. Nonaka, S. G. van Lanen, B. Shen, S. D. Bruner, *J. Am. Chem. Soc.* **2007**, *129*, 7728–7729; b) K. H. Chang, P. H. Liang, W. Beck, J. D. Scholten, D. Dunaway-Mariano, *Biochemistry* **1992**, *31*, 5605–5610.
[25] K. Zhang, K. M. Nelson, K. Bhuripanyo, K. D. Grimes, B. Zhao, C. C. Aldrich, J. Yin, *Chem. Biol.* **2013**, *20*, 92–101.
[26] a) D. J. Vollmann, L. Winand, M. Nett, *Curr. Opin. Biotechnol.* **2022**, *77*, 102761; b) L. Winand, A. Sester, M. Nett, *ChemMedChem* **2021**, *16*, 767–776.
[27] X.-j. Yue, X.-w. Cui, Z. Zhang, W.-f. Hu, Z.-f. Li, Y.-m. Zhang, Y.-z. Li, *Appl. Microbiol. Biotechnol.* **2018**, *102*, 5599–5610.
[28] D. G. Gibson, L. Young, R.-Y. Chuang, J. C. Venter, C. A. Hutchison, H. O. Smith, *Nat. Methods* **2009**, *6*, 343–345.

Manuscript received: November 4, 2022
Revised manuscript received: December 9, 2022
Accepted manuscript online: December 9, 2022
Version of record online: December 29, 2022